Article

EERI EARTHQUAKE SPECTRA

Correlations of spectral accelerations in the Chilean subduction zone

Earthquake Spectra
1–18

DOI: 10.1177/8755293019891723
journals.sagepub.com/home/eqs
SAGE

Gabriel Candia, M.EERI[1,2], Alan Poulos[2], Juan Carlos de la Llera, M.EERI[2,3], Jorge G.F. Crempien, M.EERI[2,3] and Jorge Macedo[4]

Abstract

The correlation between spectral accelerations is key in the construction of conditional mean spectra, the computation of vector-valued seismic hazard, and the assessment of seismic risk of spatially distributed systems, among other applications. Spectral correlations are highly dependent on the earthquake database used, and thus, region-specific correlation models have been developed mainly for earthquakes in western United States, Europe, Middle East, and Japan. Correlation models based on global data sets for crustal and subduction zones have also become available, but there is no consensus about their applicability on a specific region. This study proposes a new correlation model for 5% damped spectral accelerations and peak ground velocity in the Chilean subduction zone. The correlations obtained were generally higher than those observed from shallow crustal earthquakes and subduction zones such as Japan and Taiwan. The study provides two illustrative applications of the correlation model: (1) computation of conditional spectra for a firm soil site located in Santiago, Chile and (2) computation of bivariate hazard for spectral accelerations at two structural periods.

Keywords

Ground motion correlations, subduction zone earthquakes, earthquake scenarios

Date received: 6 June 2019; accepted: 23 September 2019

[1]Faculty of Civil Engineering, Universidad del Desarrollo, Santiago, Chile
[2]National Research Center for Integrated Natural Disaster Management (CIGIDEN) CONICYT/FONDAP/15110017, Santiago, Chile
[3]Department of Structural and Geotechnical Engineering, Pontificia Universidad Católica de Chile, Santiago, Chile
[4]Geosystems Engineering, Georgia Institute of Technology, Atlanta, GA, USA

Corresponding author:
Gabriel Candia, Faculty of Civil Engineering, Universidad del Desarrollo, Las Condes Av La Plaza 680, Santiago 7610658, Chile.
Email: gcandia@udd.cl

Introduction

Ground motion models (GMM) are widely used to estimate ground motion intensity measures (IMs) at a site for a given earthquake scenario. These models are semi-empirical regressions that express the *IMs* in terms of the earthquake mechanism, magnitude, site-to-source distance, and site-specific parameters, but they ignore the existing correlation between different IMs. The correlation between *IMs* is key for the implementation of vector-valued seismic hazard analysis (Bazzurro and Cornell, 2002), the development of conditional mean spectra (CMS) and conditional spectra (Lin et al., 2013), and ground motion selection techniques in general, which are based on the joint probability of occurrence of multiple *IMs*.

For an earthquake with moment magnitude M, site-to-source distance R, and other seismic parameters θ, for example, faulting mechanism or local soil conditions, the intensity measure IM can be expressed as in Equation 1 (Park et al., 2007), where $\mu_{\ln IM}(R, M, \theta)$ and σ_{lnIM} are the mean and standard deviations of the natural logarithm of IM, and the term ε, is the total residual, which is usually represented as a standard normal random variable.

$$\ln IM = \mu_{\ln IM}(R, M, \theta) + \sigma_{\ln IM}\varepsilon \tag{1}$$

Modern GMMs separate the total residual, or error, into between-events (i.e. the error component that varies from event to event), and within-event residuals (i.e. the error component that varies from record to record of the same event), as shown in Equation 2. In this equation, τ and ϕ are the between- and within-event standard deviations, respectively, and the terms η and $\hat{\varepsilon}$ are standard normal random variables. Since both errors are independent random variables, it follows necessarily that $\sigma_{\ln IM} = \sqrt{\tau^2 + \phi^2}$.

$$\ln IM = \mu_{\ln IM}(R, M, \theta) + \tau\eta + \phi\hat{\varepsilon} \tag{2}$$

Empirical evidence shows that the estimated IMs from an earthquake dataset are indeed correlated. For example, the scatter plots in Figure 1 show the relation between the observed spectral acceleration (*Sa*) values at $T_i = 0.01$ s and $T_j = 0.1$, 1.0, and 3 s using a ground motion subset of the SIBER-RISK database (SIBER-RISK, 2019); the Pearson correlation coefficients ρ between these *Sa* values are indicated at the top of the figure. Notice that $\rho = 0.94$ for the two neighboring periods 0.01 and 0.1 s, and that ρ decreases as the periods become further apart. Hence, the knowledge of *Sa* at 0.01 s provides meaningful information about *Sa* at 1.0 and 3 s.

Because ordinary GMMs provide deterministic value of the mean and standard deviation of $\ln IM$ for a given earthquake scenario, the randomness in IM comes solely from the residual (ε). Thus, a common practice has been to compute IM correlations directly from the residuals (e.g. Baker and Jayaram, 2008). To account for the independence of the error sources, Carlton and Abrahamson (2014) suggested that the total epsilon correlations at periods T_i and T_j might be computed as

$$\rho_{total}(T_i, T_j) = \frac{\tau(T_i)\tau(T_j)}{\sigma_{\ln IM}(T_i)\sigma_{\ln IM}(T_j)}\rho_B(T_i, T_j) + \frac{\phi(T_i)\phi(T_j)}{\sigma_{\ln IM}(T_i)\sigma_{\ln IM}(T_j)}\rho_W(T_i, T_j) \tag{3}$$

where $\rho_B(T_i, T_j)$ and $\rho_W(T_i, T_j)$ are the correlations of between-events and within-event residuals, respectively. Because τ values are generally smaller than ϕ values, and ρ_B and

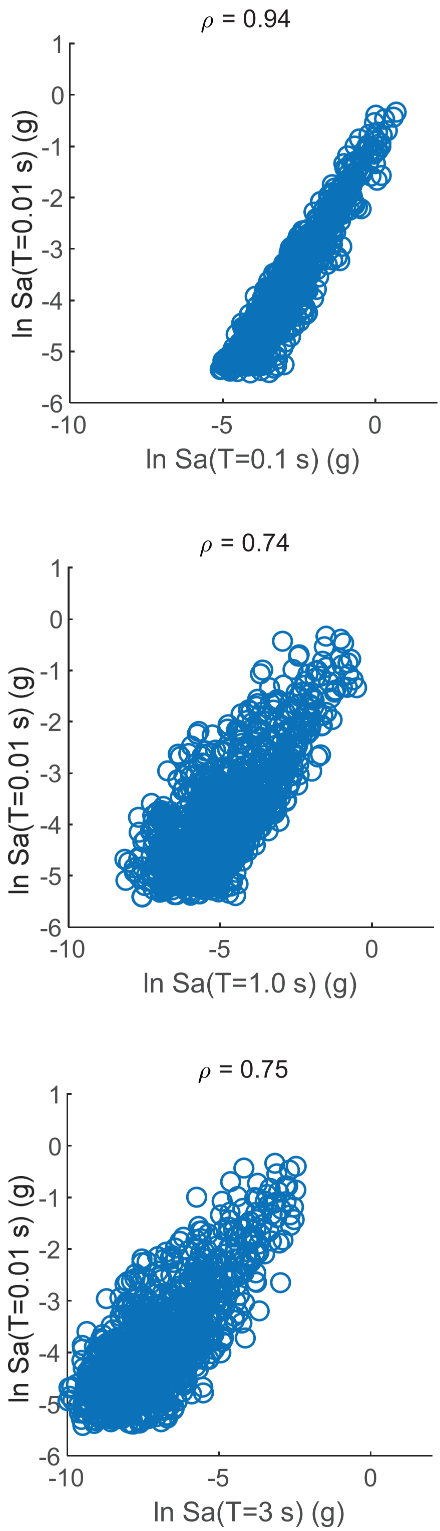

Figure 1. GMRotD50 of spectral accelerations at $T = 0.01$ s versus spectral accelerations at 0.1, 1.0, and 3.0 s computed from 97 Chilean subduction interface earthquakes.

ρ_W are similar in magnitude, the total correlations ρ_{total} are similar to the within-event correlations ρ_W.

Several studies have proposed correlation models for ground motion residuals in shallow crustal zones (e.g. Abrahamson et al., 2014; Akkar et al., 2014a; Azarbakht et al., 2014; Baker and Bradley, 2017; Baker and Cornell, 2006; Baker and Jayaram, 2008; Cimellaro, 2013; Kotha et al., 2017). Using the PEER Strong Motion Database, Baker and Cornell (2006) developed a closed-form correlation model between horizontal spectral ordinates at two different periods, a correlation model for vertical ground motions, and correlation equations for ground motion at two orthogonal directions at a single period. Later, Baker and Jayaram (2008) developed a spectral correlation model for within-event residuals using the PEER NGA database (Chiou et al., 2008), which proved valid for various definitions of spectral accelerations (i.e. the geometric mean of orthogonal components, or the geometric means GMRotDpp and GMRotIpp as defined in Boore et al., 2006). In addition, they showed that between- and within-event correlations were very similar to total correlations. Both studies concluded that correlations values are not very sensitive to the underlying GMM because correlations are controlled by variability of spectral values for different records, rather than the variability of ground motions predicted using different GMMs.

More recently, Azarbakht et al. (2014) developed a magnitude-and-distance dependent correlation model for within-event residuals based on the PEER NGA database, consisting of 1551 recordings from shallow crustal earthquakes. This study shows that the event magnitude has a marked influence on the correlation values and can affect CMS calculations. In contrast, Baker and Bradley (2017) computed correlation values for various *IMs* using the PEER NGA-West2 database (Ancheta et al., 2014), which contains 21,539 recordings from shallow crustal earthquakes. These correlations were found in excellent agreement with those obtained from alternative databases. The study concludes that correlation models are largely independent of the GMM used and earthquake parameters such as magnitude, site-to-source distance, and the average shear wave velocity on the upper 30 m, V_{S30}. They also suspect that the correlation dependency on magnitude and distance reported by Azarbakht et al. (2014) is a spurious effect due to small-sample variability and the lack of mixed-effects when computing correlations from a smaller earthquake catalog.

Other studies in active crustal regions include Ji et al. (2017), which developed a magnitude dependent model for China, and Akkar et al. (2014a) that estimated spectral correlations for Europe and the Middle East using the Pan-European RESORCE database Akkar et al. (2014b). In the work by Daneshvar et al. (2015), correlation coefficients from Eastern Canada were found significantly higher than those of Western North America (Baker and Jayaram, 2008), a result that may have been influenced by the small number of records used. More recently, a study by Kotha et al. (2017) compared correlations models derived from the PEER NGA-West2 and RESORCE databases and concluded that they are database-dependent. The authors proposed a partially non-ergodic correlation model consisting of a magnitude-dependent between-event model in conjunction with a region-dependent and site-corrected model. Although the physical explanation of the magnitude dependence of between-event residuals has not been thoroughly explored, Kotha et al. (2017) suggests that earthquakes with large magnitude and low corner frequency f_c will likely result in high *Sa* correlations at frequencies above f_c. Similar observations were made by Stafford (2017), who developed an inter frequency correlation model for Fourier spectral ordinates; this study found that between-event correlations have a mild dependence on earthquake magnitude.

Moreover, Papadopoulos et al. (2019) used the PEER NGA-West2 database to derive a closed-form model for the correlations between spectral accelerations of mainshocks and aftershock pairs. The study also found mild differences between spectral correlations at different periods within mainshock and aftershock ground motions, which do not justify the use of a separate model for each case.

In contrast to active crustal regions, fewer studies have addressed ground motion correlations for subduction zones. One of the first studies was conducted by Goda and Atkinson (2009) for Japan using the K-NET and KiK-net ground motion data. The authors computed correlation values for between-events residuals that are systematically higher than Baker and Jayaram's (2008) predictions for shallow crustal earthquakes. Likewise, Jayaram et al. (2011) computed spectral correlations for Japanese interface, slab, and crustal earthquakes, finding important statistical differences with regards to the dataset used. Abrahamson et al. (2016) computed correlation coefficients using the BC Hydro subduction zone GMM; no distinction was made between interface or slab earthquakes. Although Abrahamson et al. (2016) used global data, subduction zones other than Japan and Taiwan are underrepresented. More recently, Jaimes and Candia (2019) developed a correlation model for peak ground velocity (PGV), peak ground acceleration (PGA), and spectral accelerations (*Sa*) residuals using the SSN-UNAM dataset for Mexican interface earthquakes and rock sites. These correlation models are compared in Figure 2 for spectral accelerations residuals $\varepsilon(T_1)$ and $\varepsilon(T_2)$ with $0.1 \text{ s} \leqslant T_1 \leqslant 5 \text{ s}$ and $T_2 = 0.3$ and 3 s.

Interestingly, the subduction models by Jayaram et al. (2011) and Abrahamson et al. (2016) are in reasonable good agreement with the crustal model by Baker and Jayaram (2008), although some minor differences arise if T_1 and T_2 are far apart from one another. In contrast, Jaimes and Candia (2019) reported higher correlations than Baker and Jayaram (2008) and other subduction models. A physically sound explanation for this result remains unknown.

Recently, Carlton and Abrahamson (2014) found that hard rock sites have higher correlations at short periods, because, as the authors note, oscillator's response is controlled by the predominant period of the ground motion rather than their own natural periods. To address this problem, they proposed normalizing the periods by $T_{amp1.5}$, the shortest period at which the spectral accelerations exceed 1.5 times the PGA. The study also found that the Abrahamson and Silva (2008) correlation model for shallow crustal zones and BC Hydro's correlation model for subduction zones (Abrahamson et al., 2016) are similar because their databases share similar average $T_{amp1.5}$ values.

Pseudo acceleration response spectra, and therefore, correlations models, are very sensitive to the frequency content of the underlying ground motions. Indeed, Jayaram et al. (2011) suggested that differences between correlations from subduction and shallow crustal earthquakes may be attributed to differences in the ground motion's average frequency content. This effect, however, is masked by the inherent variability of ground motion databases.

In this study, a correlation model for spectral accelerations (*Sa*) and PGV for Chilean subduction earthquakes is proposed, based on the latest ground motion catalogs and site classification databases. The correlation model is compared to existing models for shallow crustal zones and subduction zones worldwide, and the implications of using this region-specific model in seismic hazard assessment are discussed.

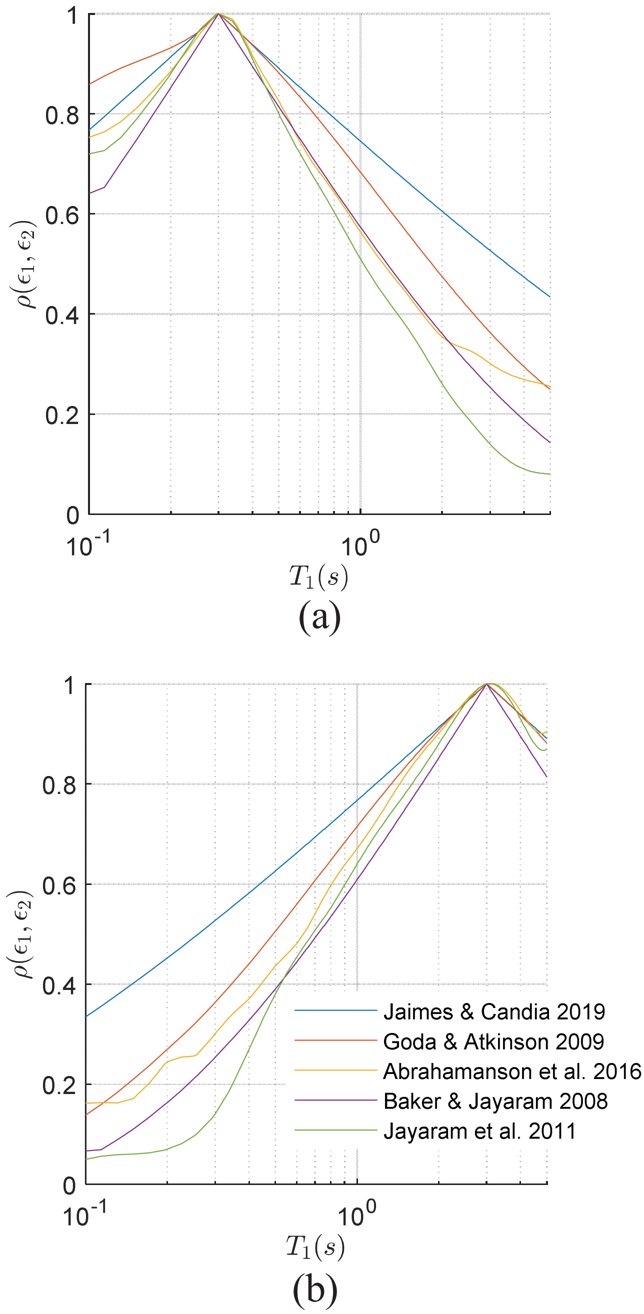

Figure 2. Comparison of correlation models for $\varepsilon(T_1)$ and $\varepsilon(T_2)$ for subduction zones and shallow crustal zones, (a) $T_2 = 0.3$ s and (b) $T_2 = 3$ s.

Strong motion database

This study uses a subset of high-quality records from the SIBER-RISK strong motion database (SIBER-RISK, 2019), which combines subduction events form the CSN

(Barrientos, 2018) and RENADIC (Bastías and Montalva, 2016) databases. The ground motions in this high-quality subset includes only earthquakes with moment magnitude $M \geqslant 5.0$, site-to-source distance up to 300 km, and records obtained at sites with $V_{s30} \geqslant 360$ m/s. Recordings from stations without proper V_{S30} characterization were removed from the analysis. A total of 1327 tri-axial records from 234 interface earthquakes, and 338 tri-axial recordings from 123 intermediate depth earthquakes are used herein. The magnitude and distance distribution of the selected ground motions from the two source types are shown in Figure 3, and the site class distribution is presented in Table 1.

To remove spurious low frequency accelerations base shifts, a third-order bandpass Butterworth filter with corner frequencies at 0.01 and 50 Hz was applied to the acceleration records. The resulting broadband acceleration records were integrated to velocity, which trace typically drifts from the zero baseline. These drifts were removed by subtracting a piecewise-linear function to the data using a reversible jump Markov Chain Monte Carlo algorithm (Sambridge et al., 2006); this approach avoids over-constraining the velocity time-series. Finally, the corrected accelerations were computed by numerically differentiating the corrected velocities with respect to time. Using the corrected data, we computed the 5% damped spectral accelerations and PGV (GMRotD50 as defined in Boore et al., 2006) for the horizontal components, in accordance with the most recent subduction zone GMMs.

The mean and standard deviation terms of Equation 1 were estimated using the GMMs for subduction zones proposed by Abrahamson et al. (2016) (BC Hydro) and Montalva et al. (2017). Interestingly, the total errors for our database have a non-negligible magnitude bias, particularly in the low magnitude range. To resolve this issue, we adopted BC Hydro's functional form (refer to Equation 1 in Abrahamson et al. 2016) and recalibrated the path scaling parameters θ_1, θ_2, θ_6, the magnitude scaling parameter θ_{13}, and depth parameter θ_{11}. For the case of interface earthquakes, notice the existence of two magnitudes groups: one with $M \leqslant 7.0$ (1191 events), and the other with $M \geqslant 7.5$ (136 events). For each group, separate sets of parameters were obtained. The remaining terms, including the site amplification terms, were set equal to those in the original BC Hydro formulation. Using a similar functional form, PGV coefficients were estimated with an analogous procedure.

Finally, a mixed-effect nonlinear regression model was used to separate the total residuals into between- and within-event residuals, with their corresponding standard deviations as shown in Figure 4. A summary of the recalibrated coefficients of the regression is shown in Supplemental Tables A1 and A2 for subduction interface earthquakes, and Supplemental Table A3 for intermediate depth earthquakes. It is apparent from the figure that between-event standard deviation τ, tend to be higher for the interface ground motions than the intermediate depth ones, while the within-event standard deviation ϕ is similar in both cases.

Correlation analysis: results and discussion

This section describes the correlation analysis developed for spectral acceleration values (5% damped GMRotD50) with period range between 0.01 and 10 s, and for PGV (GMRotD50). The total correlation $\rho_{total}(T_i, T_j)$ between the $Sa(T_i)$ and $Sa(T_j)$ residuals was computed using Equation 3, where the terms ρ_B and ρ_W correspond to the Pearson product-moment correlation of between-events and within-event residuals, respectively. These correlations are defined as the covariance of the residuals divided by the product of

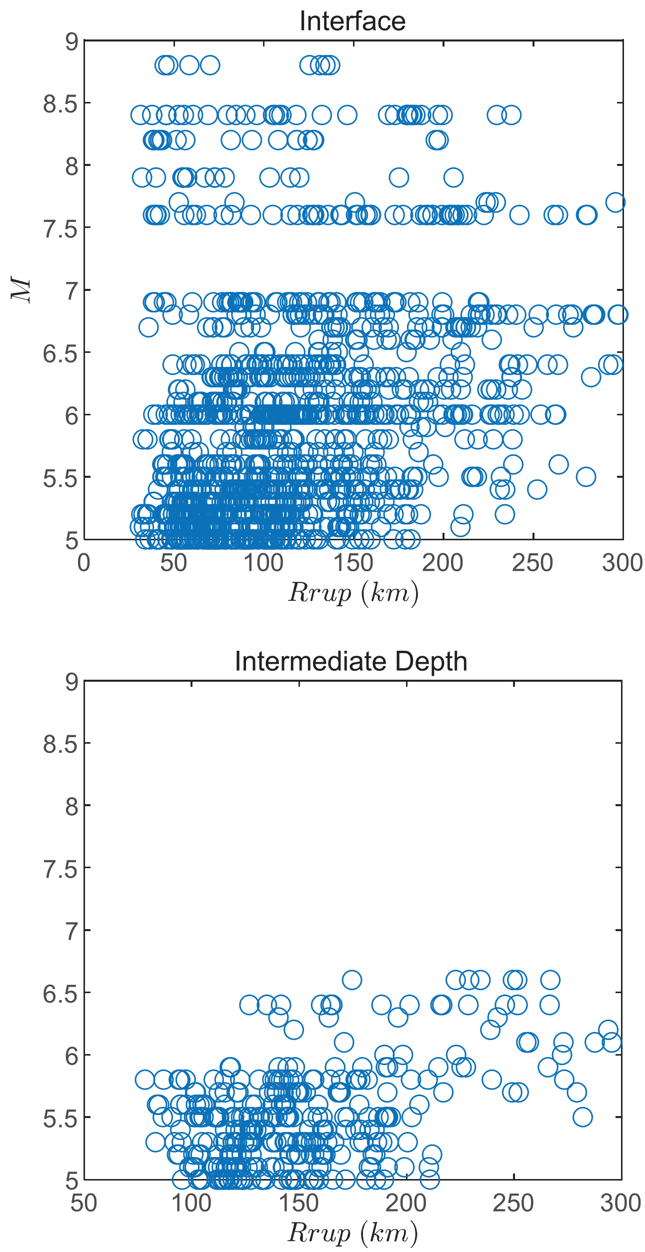

Figure 3. Magnitude versus rupture distance of selected interface and intermediate depth ground motions.

Table 1. Number of records used classified by site class.

NEHRP site class	V_{S30} (m/s)	Interface recordings	Intermediate depth recordings
A	>1500	26	4
B	760–1500	257	73
C	360–760	1044	261
Total		1327	338

NEHRP: National Earthquake Hazards Reduction Program

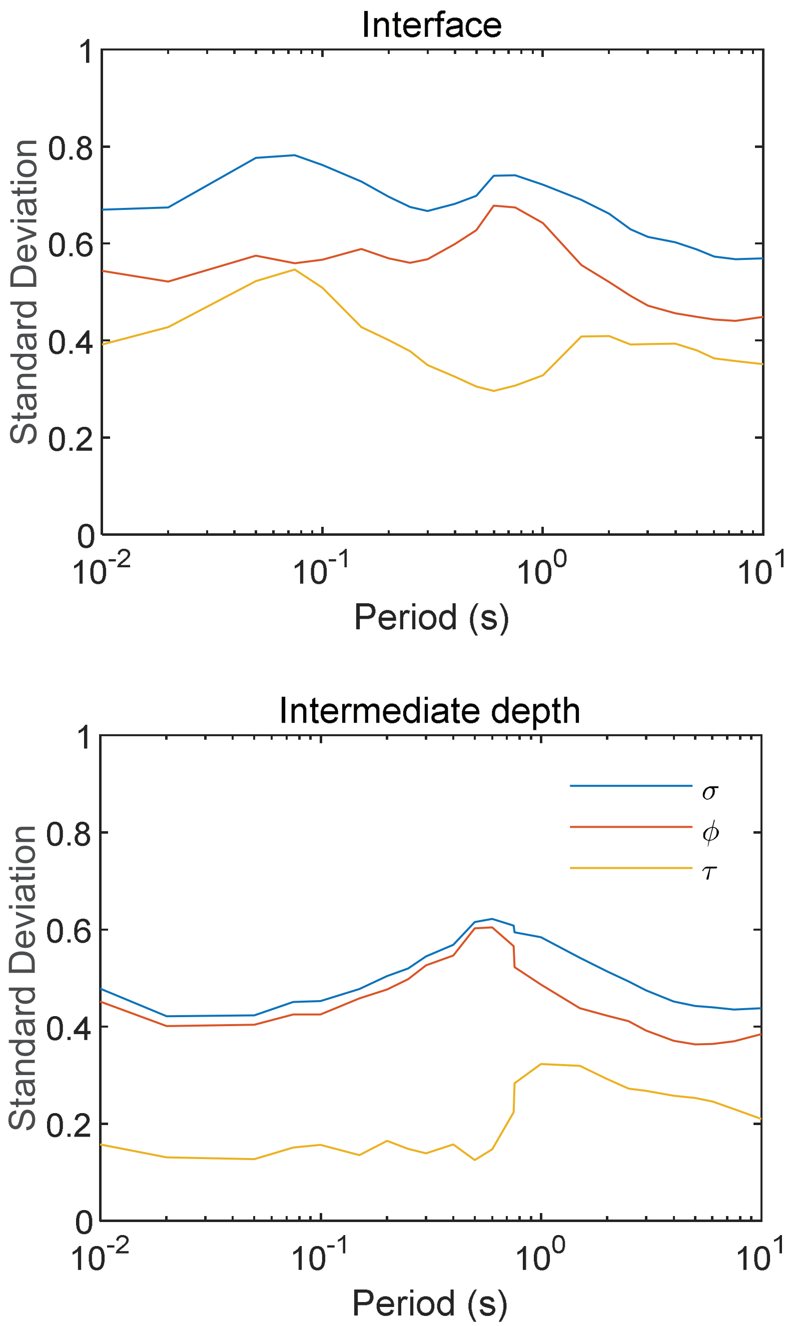

Figure 4. Total, within-event, and between-event standard deviations of *Sa* values (GMRotD50, 5% damped) computed from the HQ SIBER-RISK database and the BC Hydro's functional form.

their standard deviations. More concisely, the correlation (ρ_B or ρ_W) between all spectral acceleration pairs can be written in matrix form as shown in Equation 4, where $\mathbf{\Sigma}$ is a diagonal matrix of the standard deviations and $\mathbf{C}$ is the covariance matrix.

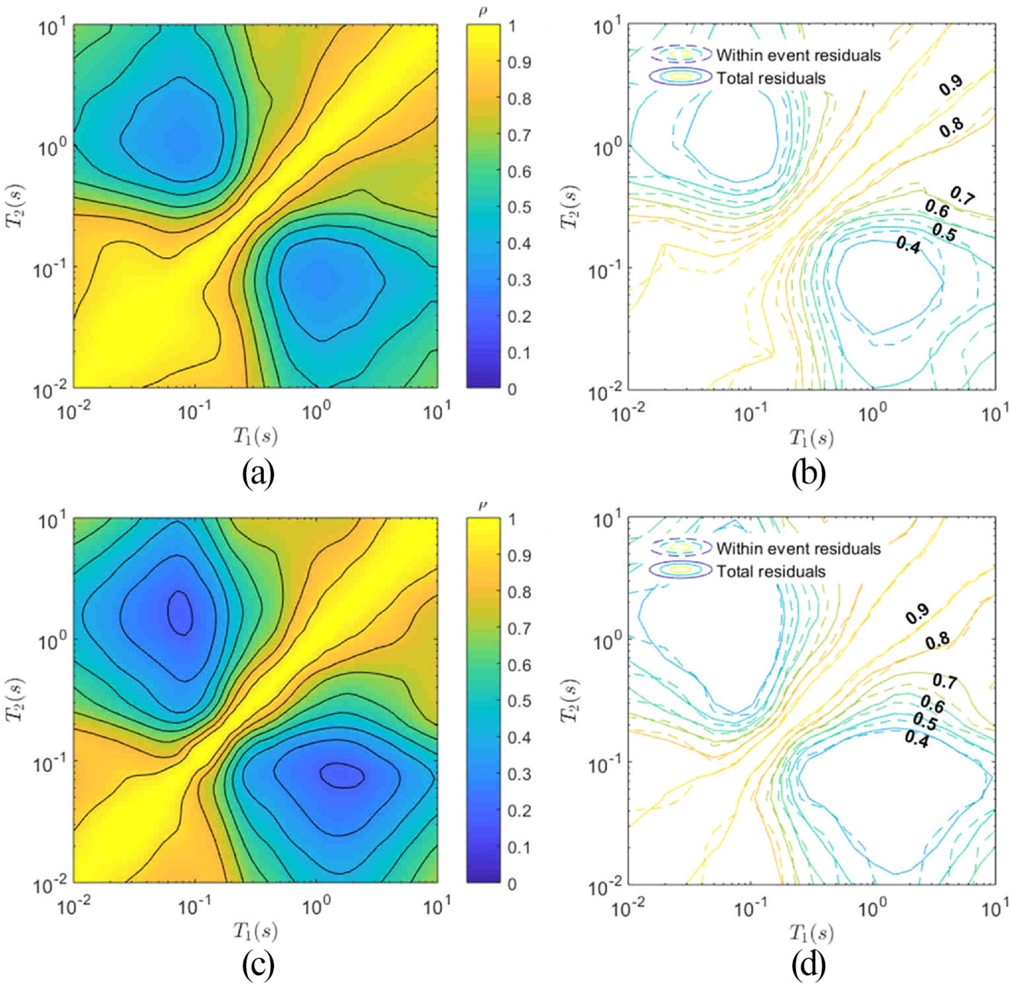

Figure 5. Contours of total residual correlations for (a) interface events, and (c) intermediate depth events, and comparison between total- and within-event residuals for (b) interface events, and (d) intermediate depth events.

$$\boldsymbol{\rho} = \boldsymbol{\Sigma}^{-1}\mathbf{C}\boldsymbol{\Sigma}^{-1} \tag{4}$$

Different ground motion subsets were used to test the dependency of the correlation structure on different variables, including magnitude and site-to-source distance, the effect of site class using V_{S30}, the number of samples in the ground motion catalog, and the effects of the assumed GMM. The resulting correlation model is shown graphically in Figure 5a and c for interface and intermediate depth earthquakes, respectively; this model is a function of spectral periods T_1 and T_2 and has important statistical differences with other subduction zone models. Since ϕ's are larger than $\tau's$, it is verified that the correlation structure of total and within-event residuals are very similar as shown in Figure 5b and d.

From Figure 5a and c, it is apparent that correlations from a given pair $(Sa(T_i), Sa(T_j))$ from interface earthquakes are slightly higher than those of intermediate depth earthquakes. Although having a separate model for different focal mechanism may not be justified in some cases, look-up tables for between-event, within-event, and total correlations are provided in the Supplemental Tables A4 and A5.

Dependence of correlation on GMM, sample size, and V_{S30}

As concluded in previous studies (e.g. Baker and Bradley, 2017; Baker and Jayaram, 2008), the underlying GMM has a minor influence on spectral correlations, which are rather controlled by the variability of the ground motion dataset. As shown in Figure 6a, three different GMMs for subduction interface earthquakes (Abrahamson et al., 2016; Montalva et al., 2017, and the modified BC Hydro model used in this study) result in very similar correlation values, with small discrepancies being our model a lower correlation bound in most cases. Analogously, correlation values were found largely independent of the site-class based on V_{S30}.

The number of ground motions (N) used to compute spectral correlations has a marked influence on the results. For instance, the correlation and the 95% confidence intervals ($CI = \pm 1.96\sigma$, with $\sigma = (1 - \rho^2)(N - 1)^{-0.5}$ as in Kotha et al., 2017) are shown in Figure 6b for interface earthquakes ($N = 1327$) and in Figure 6c for intermediate depth earthquakes ($N = 338$). From these figures, it is apparent that the CI for subduction events is well constrained due to the large number of records used. On the other hand, a larger uncertainty is observed in the correlation model for intermediate depth events, which can be significant in some application.

Comparison with previous models

Spectral pseudo acceleration correlations derived from the SIBER-RISK database are generally higher than correlations obtained for Japan (Jayaram et al., 2011) and global data (Abrahamson et al., 2016) as shown in Figure 7. From the top row plots, it comes to our attention that the correlation values for $T_1 > 1.5\,s$ increase significantly compared to other correlation models. In some cases, these differences can be important; for instance, for $T_1 = 3\,s$ and $T_2 = 0.3\,s$ (upper right plot) Jayaram et al. (2011) predicts $\rho = 0.14$, whereas in the current model $\rho = 0.66$. Large correlation values between distant periods were also observed by Jaimes and Candia (2019) using the SSN-UNAM database for Mexican interface earthquakes. However, the reason for this apparent discrepancy is unclear yet. After an extensive search of the possible causes, we still cannot provide a sound physics-based argument to support it. We suspect that using V_{S30} as a proxy for site amplification may not be appropriate at several of the recording stations; more research is needed to confirm this. We have decided to draw this as a dash line in order to caution the reader.

Total correlation values for PGV and Sa residuals computed from the SIBER-RISK database are shown in Figure 8. Notice that for both interface and intermediate depth mechanisms, the PGV correlations for the Chilean subduction zone are approximately constant, with average values between 0.65 and 0.80. This result is consistent with PGV models for Mexican interface earthquakes, and the PEER NGA and PEER NGA-West2 data.

Implications for conditional spectra

One of the most common application of IM correlation structures is the computation of CMS (e.g. Carlton and Abrahamson, 2014), and Conditional Spectra, CS (Lin et al.,

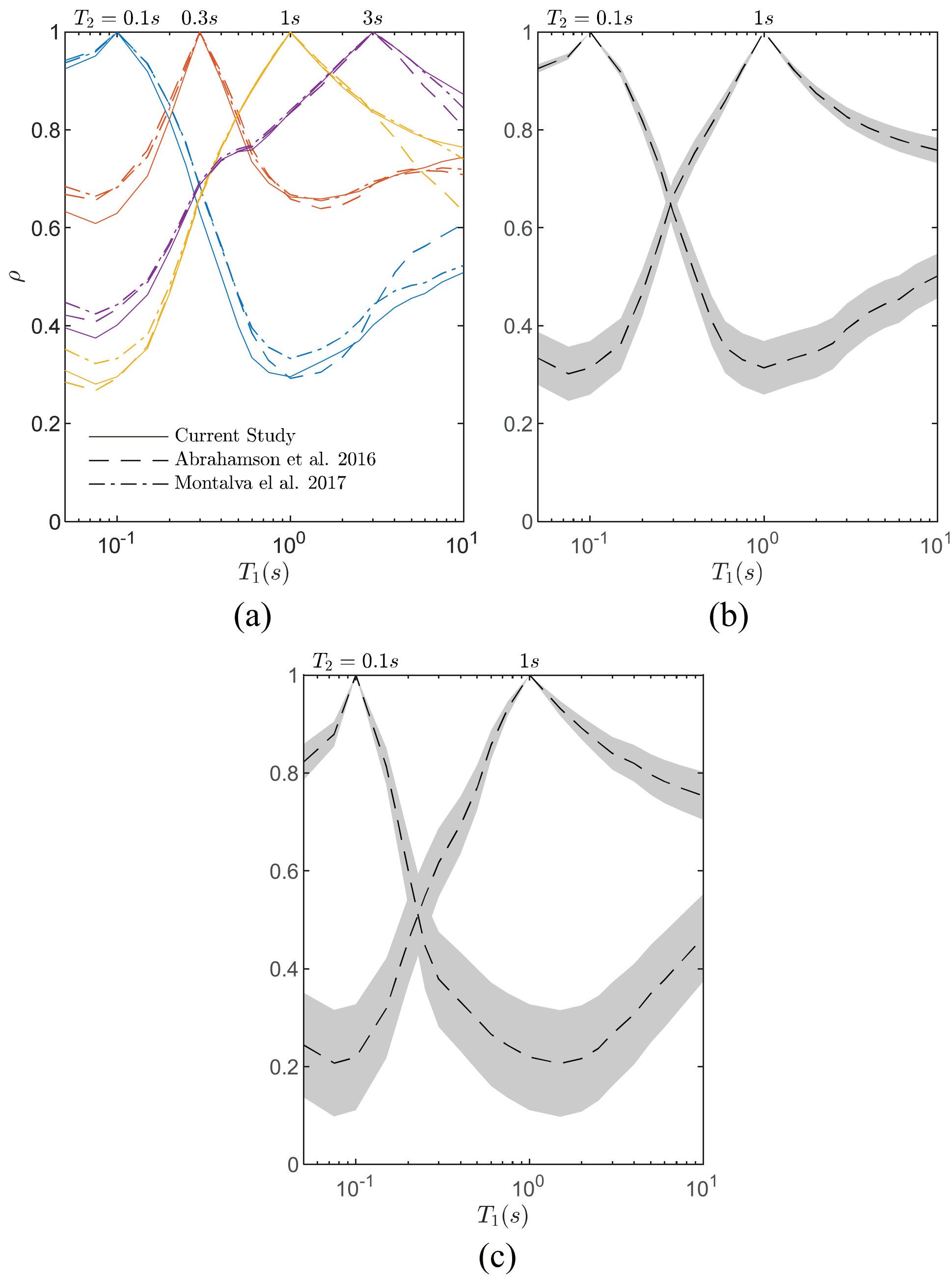

Figure 6. Spectral correlations computed for interface earthquakes: (a) influence of ground motion model on the correlation, (b) *Sa* correlations and 95% confidence interval for subduction interface events, and (c) *Sa* correlations and 95% confidence interval for intermediate depth events.

2013). In the following example, a suite of CSs is computed for a firm soil site located in Santiago; the analysis considers the seismic source model of Poulos et al. (2019), and our GMM adjusted for the SIBER-RISK database, as described previously. For conditioning periods $T^* = 0.1, 0.3$, and 1.0 s, the design accelerations associated with a 475-year return

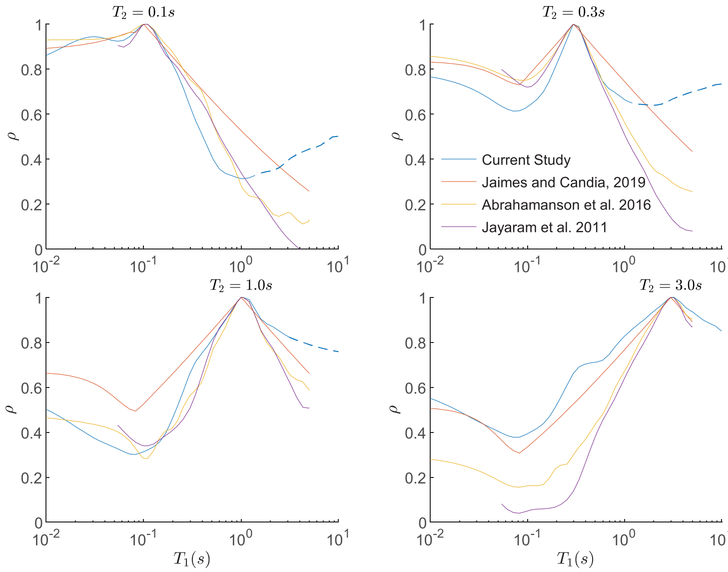

Figure 7. Comparison of computed spectral correlations with alternative interface subduction models. The correlation values in the dashed line deserve further research.

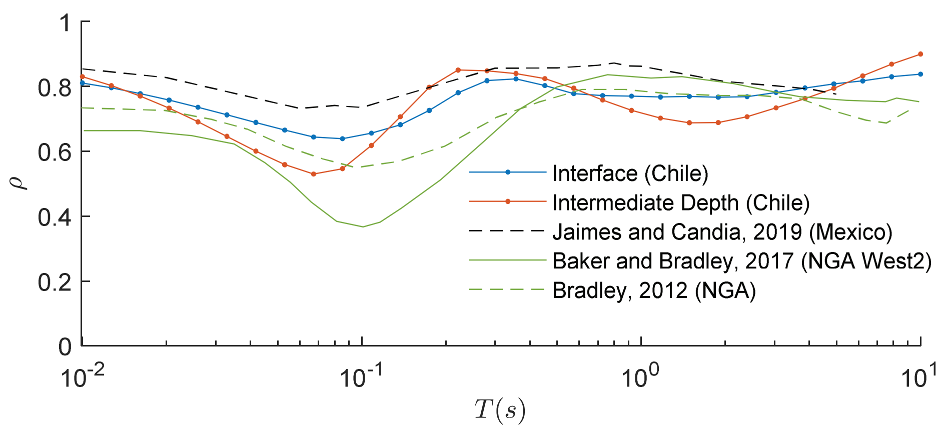

Figure 8. Correlation coefficient between PGV and *Sa* values.

period are 0.86, 0.81, and 0.26 g, respectively. Figure 9 shows the comparison of the CS obtained using the proposed correlation model for Chile and that of Abrahamson et al. (2016) for global data. The figure also presents the magnitude, rupture distance, and ε value of each case. Interestingly, despite the differences in the form of the correlation structure $\rho(T, T^*)$, the resulting CSs are very similar. As expected, and based on Figure 7, the largest differences occur for $T^* = 0.3$ s and for natural periods above 2 s (Figure 9b). For many practical purposes, the differences between these CSs are not very significant. Baker and Bradley (2017) reported similar results; the authors found no significant differences in the CSs computed from differing correlation models.

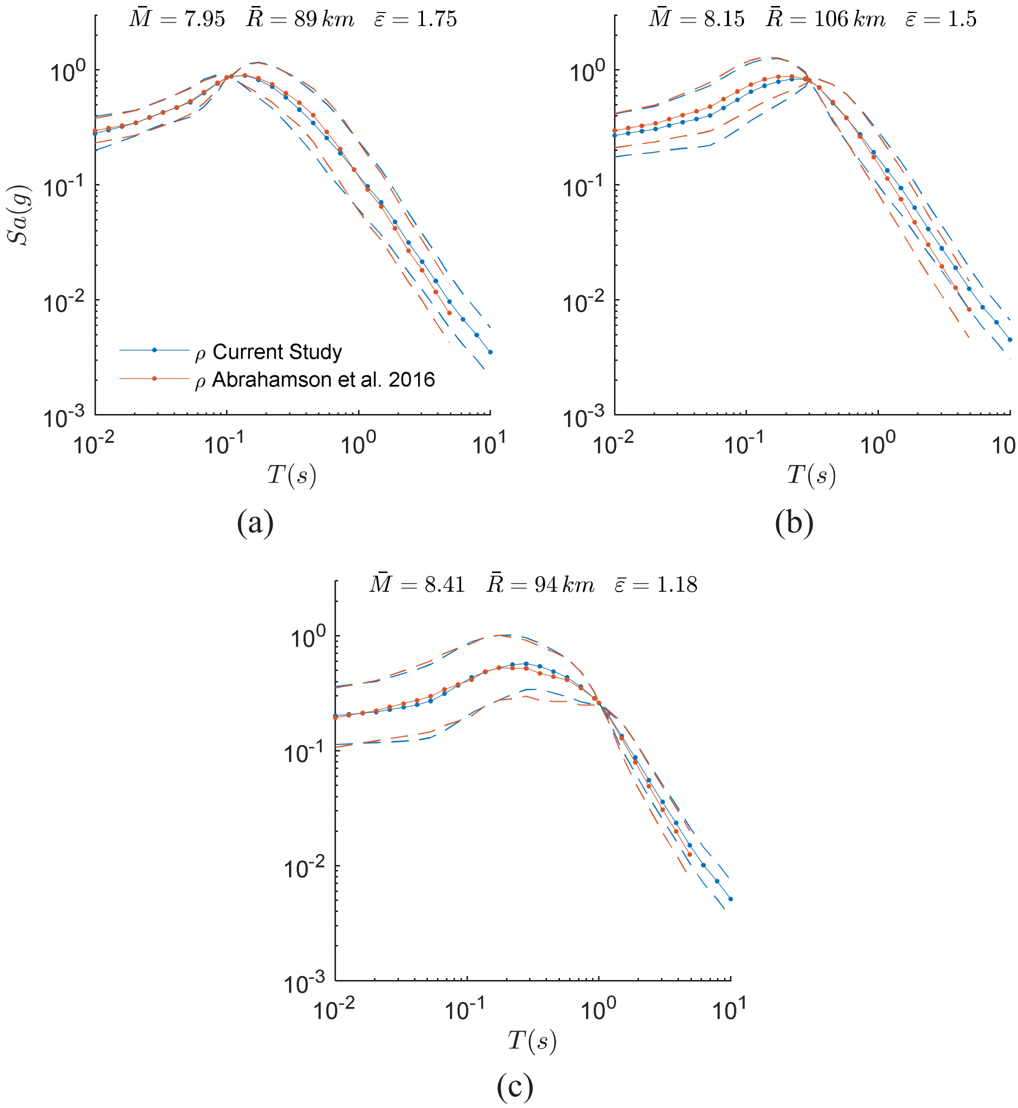

Figure 9. Examples of Conditional Spectra (CS) computed for three conditioning periods: (a) $T^* = 0.1$ s; $T^* = 0.3$ s, and (c) $T^* = 1.0$ s. Solid dotted lines are the CMS; dashed lines are the conditional mean $\pm$ one standard deviation (of ln *Sa*).

Implications for vector-valued PSHA

The following example presents the effects of three correlation values (ρ = 0, 0.30, and 0.66) on the mean rate density (MRD) function for two *IMs*, say $IM_1 = Sa(T = 0.3\,s)$ and $IM_2 = Sa(T = 3\,s)$. The Bazzurro and Cornell (2002) formulation for the MRD, shown in Equation 5, assumes that both *IMs* follow a bivariate lognormal distribution. The term $f_{IM_1,IM_2}(x_1, x_2|m, r)$ in Equation 5 corresponds to the joint probability density function conditioned on the scenario (m,r), and the double integral adds the contribution from all possible (m,r) scenarios to the total rate.

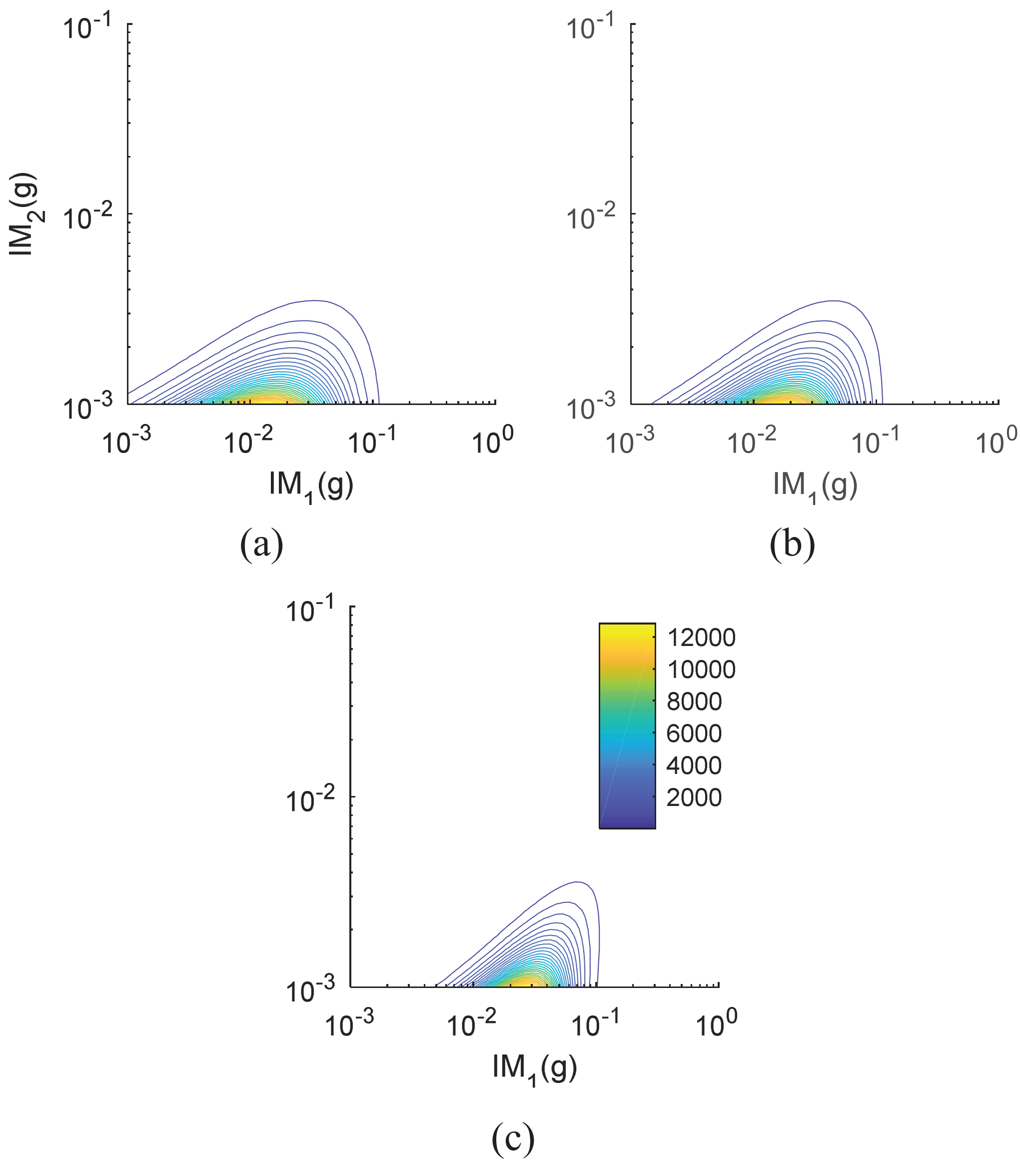

Figure 10. Contours of MRD for $IM_1 = Sa(T = 0.3\,s)$ and $IM_2 = Sa(T = 3\,s)$; (a) No correlation considered, (b) $\rho = 0.30$ as per Abrahamson et al., 2016, and (c) $\rho = 0.66$ based on the current model.

$$MRD_{IM_1,IM_2}(x_1, x_2) = \sum_{i=1}^{nSources} \nu_i \left\{ \iint f_{IM_1,IM_2}(x_1, x_2|m, r) f_{M,R}(m, r) dm dr \right\}_i \tag{5}$$

This example considers the interface and intermediate-depth sources defined by Poulos et al. (2019), the recalibrated BC Hydro GMM discussed earlier, and circular rupture areas within each seismic source. The results in Figure 10 show that as ρ increases, the bivariate distribution becomes narrower, and the dominant rates concentrate along an oblique band.

Consequently, the correct choice of ρ influences the generation of ground motion scenarios sampled from f_{IM_1,IM_2}, and hence, it affects risk computations.

Conclusion

The current study presents correlations for 5% damped spectral pseudo accelerations at different periods and PGV (GMRotD50) for Chilean subduction earthquakes. The model was developed using a high-quality dataset of 1327 interface ground motions and 338 intermediate depth ground motions recorded predominantly on sites classes NEHRP B and C. Ground motion correlations were computed using the composition of between- and within-event correlations, as suggested by Carlton and Abrahamson (2014), and a database-specific GMM. Results show that interperiod correlations are largely independent of the site class based on V_{S30}, magnitude, the underlying GMM, and that standard errors of the correlations are better constrained with increasing number of recordings. Most importantly, the present study shows that inter-period correlations for the Chilean subduction zone are generally higher than predicted by the correlation models developed for Japan and Taiwan, and higher than the values of the correlation models for shallow crustal regions derived from the PEER NGA and PEER NGA-West2 datasets. A sound physics-based reason for these differences remains unknown and requires further research. In particular, the current Chilean database defines proxies for site amplification in a large number of recording stations (e.g. topographical-based V_{S30} and H/V spectral ratios), which may be have an effect in the observed correlation trends. Despite the recent advances in site characterization at ground motion stations, more research is required to constraint the site effects terms of GMMs for the local subduction zone. In addition, we speculate that basin effects within the Chilean territory and the signal processing of the low-frequency component of subduction earthquakes may have an influence on the observed patterns.

Acknowledgments

The authors are grateful for these supports. Also, we thank Sebastián Castro for his work in the curation of the SIBER- RISK database, and Dr. David Wald (ES editor), Dr. Jack Baker and one anonymous reviewer for the careful examination of the manuscript and their constructive comments.

Declaration of conflicting interests

The author(s) declared no potential conflicts of interest with respect to the research, authorship, and/or publication of this article.

Funding

The author(s) disclosed receipt of the following financial support for the research, authorship, and/or publication of this article: This research was sponsored by the National Research Center for Integrated Natural Disaster Management CONICYT/FONDAP/15110017, Facultad de Ingeniería Civil at Universidad del Desarrollo, FONDECYT Grant No. 1170836 "SIBER-RISK: SImulation Based Earthquake Risk and Resilience of Interdependent Systems and NetworKs," and FONDECYT Grant No. 11180937 "Seismic Risk of Mined Tunnels."

Supplemental material

Supplemental material for this article is available online.

References

Abrahamson N and Silva W (2008) Summary of the Abrahamson & Silva NGA ground-motion relations. *Earthquake Spectra* 24(1): 67–97.

Abrahamson N, Gregor N and Addo K (2016) BC Hydro ground motion prediction equations for subduction earthquakes. *Earthquake Spectra* 32(1): 23–44.

Abrahamson NA, Silva WJ and Kamai R (2014) Summary of the ASK14 ground motion relation for active crustal regions. *Earthquake Spectra* 30(3): 1025–1055.

Akkar S, Sandıkkaya MA and Ay BÖ (2014a) Compatible ground-motion prediction equations for damping scaling factors and vertical-to-horizontal spectral amplitude ratios for the broader Europe region. *Bulletin of Earthquake Engineering* 12(1): 517–547.

Akkar S, Sandıkkaya MA, Şenyurt M, et al. (2014b) Reference database for seismic ground-motion in Europe (RESORCE). *Bulletin of Earthquake Engineering* 12(1): 311–339.

Ancheta T, Darragh R, Stewart J, et al. (2014) NGA-West2 database. *Earthquake Spectra* 30(3): 989–1005.

Azarbakht A, Mousavi M, Nourizadeh M, et al. (2014) Dependence of correlations between spectral accelerations at multiple periods on magnitude and distance. *Earthquake Engineering & Structural Dynamics* 43(8): 1193–1204.

Baker JW and Bradley BA (2017) Intensity measure correlations observed in the NGA-West2 database, and dependence of correlations on rupture and site parameters. *Earthquake Spectra* 33(1): 145–156.

Baker JW and Cornell CA (2006) Correlation of response spectral values for multicomponent ground motions. *Bulletin of the Seismological Society of America* 96(1): 215–227.

Baker JW and Jayaram N (2008) Correlation of spectral acceleration values from NGA ground motion models. *Earthquake Spectra* 24(1): 299–317.

Barrientos S (2018) The seismic network of Chile. *Seismological Research Letters* 89(2A): 467–474.

Bastías N and Montalva GA (2016) Chile strong ground motion flatfile. *Earthquake Spectra* 32(4): 2549–2566.

Bazzurro P and Cornell CA (2002) Vector-valued probabilistic seismic hazard analysis (VPSHA). In: *Proceedings of the 7th U.S. national conference on earthquake engineering*, Boston, MA, 21–25 July.

Boore DM, Watson-Lamprey J and Abrahamson NA (2006) Orientation-independent measures of ground motion. *Bulletin of the Seismological Society of America* 96(4A): 1502–1511.

Carlton B and Abrahamson N (2014) Issues and approaches for implementing conditional mean spectra in practice. *Bulletin of the Seismological Society of America* 104(1): 503–512.

Chiou B, Darragh R, Gregor N, et al. (2008) NGA project strong-motion database. *Earthquake Spectra* 24(1): 23–44.

Cimellaro GP (2013) Correlation in spectral accelerations for earthquakes in Europe. *Earthquake Engineering & Structural Dynamics* 42(4): 623–633.

Daneshvar P, Bouaanani N and Godia A (2015) On computation of conditional mean spectrum in eastern Canada. *Journal of Seismology* 19(2): 443–467.

Goda K and Atkinson GM (2009) Probabilistic characterization of spatially correlated response spectra for earthquakes in Japan. *Bulletin of the Seismological Society of America* 99(5): 3003–3020.

Jaimes MA and Candia G (2019) Interperiod correlation model for Mexican interface earthquakes. *Earthquake Spectra* 35(3): 1351–1365.

Jayaram N, Baker JW, Okano H, et al. (2011) Correlation of response spectral values in Japanese ground motions. *Earthquake and Structures* 2(4): 357–376.

Ji K, Bouaanani N, Wen R, et al. (2017) Correlation of spectral accelerations for earthquakes in China. *Bulletin of the Seismological Society of America* 107(3): 1213–1226.

Kotha SR, Bindi D and Cotton F (2017) Site-corrected magnitude- and region-dependent correlations of horizontal peak spectral amplitudes. *Earthquake Spectra* 33(4): 1415–1432.

Lin T, Harmsen SC, Baker JW, et al. (2013) Conditional spectrum computation incorporating multiple causal earthquakes and ground-motion prediction models. *Bulletin of the Seismological Society of America* 103(2A): 1103–1116.

Montalva, G. A., N. Bastías, and A. Rodríguez-Marek (2017). Ground motion prediction equation for the Chilean subduction zone, *Bull. Seismol. Soc. Am.* 107, no. 2, 901–911.

Papadopoulos AN, Kohrangi M and Bazzurro P (2019) Correlation of spectral acceleration values of mainshock-aftershock ground motion Pairs. *Earthquake Spectra* 35(1): 39–60.

Park J, Bazzurro P and Baker JW (2007) Modeling spatial correlation of ground motion intensity measures for regional seismic hazard and portfolio loss estimation. In: Kanda J, Takada T and Furuta H (eds) *Applications of Statistics and Probability in Civil Engineering*: 1–8. London: Taylor & Francis.

Poulos A, Monsalve M, Zamora N, et al. (2019) An updated recurrence model for Chilean subduction seismicity and statistical validation of its Poisson nature. *Bulletin of the Seismological Society of America* 109(1): 66–74.

Sambridge M, Gallagher K, Jackson A, et al. (2006) Trans-dimensional inverse problems, model comparison and the evidence. *Geophysical Journal International* 167(2): 528–542.

SIBER-RISK (2019) SIBER-RISK strong motion database. Available at: https://siberrisk.ing.puc.cl/StrongMotionDatabase (accessed 6 September 2019).

Stafford PJ (2017) Interfrequency correlations among Fourier spectral ordinates and implications for stochastic ground-motion simulation. *Bulletin of the Seismological Society of America* 107(6): 2774–2791.